BAR EVOLUTION OVER THE LAST 8 BILLION YEARS: A CONSTANT FRACTION OF STRONG BARS IN THE GEMS SURVEY

SHARDHA JOGEE,[1] FABIO D. BARAZZA,[1] HANS-WALTER RIX,[2] ISAAC SHLOSMAN,[3] MARCO BARDEN,[2] CHRISTIAN WOLF,[4] JAMES DAVIES,[1] INGE HEYER,[1] STEVEN V.W. BECKWITH,[1,5] ERIC F. BELL,[2] ANDREA BORCH,[2] JOHN A. R. CALDWELL,[1] CHRISTOPHER J. CONSELICE,[6] TOMAS DAHLEN,[1] BORIS HÄUSSLER,[2] CATHERINE HEYMANS,[2] KNUD JAHNKE,[7] JOHAN H. KNAPEN,[8] SEPPO LAINE,[9] GABRIEL M. LUBELL,[10] BAHRAM MOBASHER,[1] DANIEL H. MCINTOSH[11] KLAUS MEISENHEIMER,[2] CHIEN Y. PENG,[12] SWARA RAVINDRANATH,[1] SEBASTIAN F. SANCHEZ,[7] RACHEL S. SOMERVILLE,[1] AND LUTZ WISOTZKI[7]

ABSTRACT

One-third of present-day spirals host optically visible strong bars that drive their dynamical evolution. However, the fundamental question of how bars evolve over cosmological times has yet to be resolved, and even the frequency of bars at intermediate redshifts remains controversial. We investigate the frequency of bars out to $z \sim 1$ drawing on a sample of 1590 galaxies from the Galaxy Evolution from Morphologies and SEDs survey, which provides morphologies from *Hubble Space Telescope* Advanced Camera for Surveys (ACS) two-band images and accurate redshifts from the COMBO-17 survey. We identify spiral galaxies using three independent techniques based on the Sersic index, concentration parameter, and rest-frame color. We characterize bar and disk features by fitting ellipses to F606W and F850LP images, using the two bands to minimize shifts in the rest-frame bandpass. We exclude highly inclined ($i > 60°$) galaxies to ensure reliable morphological classifications and apply different completeness cuts of $M_V \leq -19.3$ and -20.6. More than 40% of the bars that we detect have semimajor axes $a < 0\farcs5$ and would be easily missed in earlier surveys without the small point-spread function of ACS. The bars that we can reliably detect are fairly strong (with ellipticities $e \geq 0.4$) and have a in the range $\sim1.2–13$ kpc. We find that the optical fraction of such strong bars remains at $\sim30\% \pm 6\%$ from the present day out to look-back times of 2–6 Gyr ($z \sim 0.2–0.7$) and 6–8 Gyr ($z \sim 0.7–1.0$); it certainly shows no sign of a drastic decline at $z > 0.7$. Our findings of a large and similar bar fraction at these three epochs favor scenarios in which cold gravitationally unstable disks are already in place by $z \sim 1$ and where on average bars have a long lifetime (well in excess of 2 Gyr). The distributions of structural bar properties in the two slices are, however, not statistically identical and therefore allow for the possibility that the bar strengths and sizes may evolve over time.

Subject headings: galaxies: evolution — galaxies: general — galaxies: spiral — galaxies: structure

1. INTRODUCTION

It is widely recognized that stellar bars, either spontaneously or tidally induced, redistribute mass and angular momentum and thereby drive the dynamical and secular evolution of galaxies (e.g., Kormendy 1982; Shlosman et al. 1989; Pfenniger & Norman 1990; Friedli & Benz 1993; Kormendy & Kennicutt 2004). In the local universe, one-third of local spiral galaxies host optically visible strong bars (e.g., Eskridge et al. 2002, hereafter E02; see also § 3). Mounting evidence, including observations of central molecular gas concentrations (e.g., Sakamoto et al. 1999), velocity fields (e.g., Regan et al. 1997), and starbursts (e.g., Hunt & Malkan 1999; Jogee et al. 2004a), suggests that bars strongly influence their host galaxies. However, the most fundamental issues have yet to be resolved. When and how did

bars form? Are bars a recent phenomenon, or were they abundant at early cosmic epochs? Are bars long-lived, or do they recurrently dissolve and reform over a Hubble time? How do stellar bars fit within the hierarchical clustering framework of galaxy evolution and relate to the underlying disk evolution?

The evolution of a bar over a Hubble time depends on the host galaxy structure, the dark matter (DM) halo, and the environment. Numerical simulations of this complex process make widely different predictions (e.g., Friedli & Benz 1993; Shlosman & Noguchi 1993; El-Zant & Shlosman 2002; Athanassoula 2002; Bournaud & Combes 2002; Shen & Sellwood 2004), while the handful of observational results on bars at intermediate redshifts are conflicting. On the basis of 46 moderately inclined galaxies imaged with the Wide Field Planetary Camera 2 (WFPC2) in the Hubble Deep Field (HDF), Abraham et al. (1999, hereafter A99) claim a dramatic decline in the rest-frame optical bar fraction (f_{opt}) from $\sim24\%$ at $z \sim 0.2–0.7$ to below 5% at $z > 0.7$. On the basis of Near-Infrared Camera and Multi-Object Spectrometer (NICMOS) images of 95 galaxies in the HDF at $z \sim 0.7–1.1$, Sheth et al. (2003, hereafter S03) detect four large bars with mean semimajor axes a of 12 kpc ($1\farcs4$), while smaller bars presumably escaped detection because of the large NICMOS point-spread function (PSF). S03 point out that their observed bar fraction of $\sim5\%$ for large (12 kpc) bars at $z > 0.7$ is at least comparable to the local fraction of similarly large bars. From a study based on *Hubble Space Telescope* (*HST*) Advanced Camera for Surveys (ACS) F814W images of 186 galaxies over a $3\farcm9 \times 4\farcm2$ area in the

[1] Space Telescope Science Institute, 3700 San Martin Drive, Baltimore, MD 21218; jogee@stsci.edu.

[2] Max-Planck Institute for Astronomy, D-69117 Heidelberg, Germany.

[3] University of Kentucky, Lexington, KY 40506-0055.

[4] Astrophysics, University of Oxford, Oxford OX1 3RH, UK.

[5] Johns Hopkins University, Charles and 4th Street, Baltimore, MD 21218.

[6] Department of Astronomy, California Institute of Technology, Pasadena, CA 91125.

[7] Astrophysikalisches Institut Potsdam, D-14482 Potsdam, Germany.

[8] University of Hertfordshire, Hatfield, Herts AL10 9AB, UK.

[9] *Spitzer* Science Center, California Institute of Technology, Mail Code 220-6, 1200 East California Boulevard, Pasadena, CA 91125.

[10] Vassar College, Poughkeepsie, NY 12604.

[11] University of Massachusetts, Amherst, MA 01003.

[12] University of Arizona, Tucson, AZ 85721.

TABLE 1
OPTICAL FRACTION $f_{\rm opt}$ OF STRONG ($e \geq 0.4$) BARS AT $0.25 < z \leq 0.70$ ($T_{\rm back} \sim 2$–6 Gyr) AND $0.7 < z \leq 1.0$ ($T_{\rm back} \sim 6$–8 Gyr)

Redshift Range (1)	$N_{\rm gal}$ (2)	Technique to Identify Disks/Spirals (3)	$N_{\rm sp/disk}$ (4)	Filter to Trace Bars (5)	Rest-Frame Band (6)	Optical Bar Fraction $f_{\rm opt}$ (7)

Redshift Range (1)	$N_{\rm gal}$ (2)	Technique to Identify Disks/Spirals (3)	$N_{\rm sp/disk}$ (4)	Filter to Trace Bars (5)	Rest-Frame Band (6)	Optical Bar Fraction $f_{\rm opt}$ (7)
Method I: Using the reddest ACS filter (F850LP) to identify bars						
0.25–0.70 ……	384 (146)	Sersic n	148 (39)	F850LP	I to V	36% (33%)
0.70–1.0 …….	243 (135)	Sersic n	110 (49)	F850LP	V to B	24% (27%)
0.25–0.70 ……	384 (146)	CAS C	170 (51)	F850LP	I to V	27% (27%)
0.70–1.0 …….	243 (135)	CAS C	147 (73)	F850LP	V to B	23% (23%)
0.25–0.70 ……	384 (146)	$U-V$	175 (51)	F850LP	I to V	29% (28%)
0.70–1.0 …….	243 (135)	$U-V$	139 (69)	F850LP	V to B	29% (26%)
Method II: Using F606W and F850LP to identify bars at an approximately fixed rest-frame B/V band						
0.25–0.70 ……	384 (146)	Sersic n	148 (39)	F606W	V to B	26% (30%)
0.70–1.0 …….	243 (135)	Sersic n	110 (49)	F850LP	V to B	24% (27%)
0.25–0.70 ……	384 (146)	CAS C	170 (51)	F606W	V to B	24% (28%)
0.70–1.0 …….	243 (135)	CAS C	147 (73)	F850LP	V to B	23% (23%)
0.25–0.70 ……	384 (146)	$U-V$	175 (51)	F606W	V to B	29% (23%)
0.70–1.0 …….	243 (135)	$U-V$	139 (69)	F850LP	V to B	29% (26%)

NOTES.—Col. (1): The redshift range. Col. (2): The number of galaxies in this range with $M_V \leq -19.3$ and -20.6 (shown in parentheses) to which ellipses were fitted. Col. (3): The technique used to identify disk/spiral galaxies from the sample in col. (2). We use cuts of Sersic index $n < 2.5$, CAS concentration index $C < 3.4$, and rest-frame $U - V < 0.8$–1.2. Col. (4): $N_{\rm sp/disk}$, the number of moderately inclined ($i < 60°$) spiral/disk galaxies for the two magnitude cuts in col. (2). Cols. (5) and (6): The filter and rest-frame band in which bars are traced. Col. (7): $f_{\rm opt}$, the optical fraction of strong bars, is the fraction ($N_{\rm bar}/N_{\rm sp/disk}$) of moderately inclined spirals hosting bars with $e \geq 0.4$. Values for the two magnitude cuts of -19.3 and -20.6 are shown.

Tadpole field, Elmegreen et al. (2004, hereafter E04) report a constant optical bar fraction of ~20%–40% at $z \sim 0$–1.1. This study is limited by the large (0.1–0.4) errors of the photometric redshifts (Benítez et al. 2004), and the small sample size precludes absolute magnitude completeness cuts. Furthermore, with only a single ACS filter, the rest-frame bandpass of the observations shifts by more than a factor of 2 over $z \sim 0$–1.1.

In this Letter (Paper I; see also Jogee et al. 2004b), we present the first results of an extensive study of bars at $z \sim 0.2$–1.0, based on two-band ACS images covering $14' \times 14'$ (~25%) of the Galaxy Evolution from Morphologies and SEDs (GEMS) survey. The area and the sample size of 1590 galaxies provide at least an order of magnitude better number statistics than earlier studies. We quantitatively identify bars using ellipse fits and minimize the effects of bandpass shifts by using both F850LP and F606W images (§ 2.2). Using highly accurate redshifts (§ 2.1), we compare the bar fractions in two redshift slices after applying completeness criteria. We show that the optical fraction of strong (ellipticities $e \geq 0.4$) bars is remarkably constant (~30%) from the present-day out to look-back times ($T_{\rm back}$) of 2–6 Gyr ($z \sim 0.2$–0.7)[13] and 6–8 Gyr ($z \sim 0.7$–1.0).

2. OBSERVATIONS, SAMPLE, AND METHODOLOGY

2.1. Observations and Sample Selection

GEMS is a two-band (F606W and F850LP) *HST* ACS imaging survey (Rix et al. 2004) of an 800 arcmin^2 (~$28' \times 28'$) field centered on the Chandra Deep Field–South. GEMS consists of 78 one-orbit–long ACS pointings in each filter and reaches a limiting 5 σ depth for point sources of 28.3 and 27.1 AB mag in F606W and F850LP, respectively. GEMS provides high-resolution (~0″.05 or 360 pc at $z \sim 0.7$) ACS images for ~8300 galaxies in the redshift range $z \sim 0.2$–1.1, where accurate redshifts [$\delta_z/(1 + z) \sim 0.02$ down to $R_{\rm Vega} = 24$] and spectral energy distributions (SEDs) based on 17 filters exist from the COMBO-17 project (Wolf et al. 2004). For this Letter, we analyze only ~25% of the GEMS field, as this area ($14' \times 14'$) is already 30 times that of the HDF and yields good number statistics and robust results on the bar fraction (§ 3). It provides a sample that consists of 1590 galaxies in the

range $z \sim 0.2$–1.0 and $R_{\rm Vega} \leq 24$. In a future paper (S. Jogee et al. 2004, in preparation, hereafter Paper II), we will use the entire GEMS sample to compare how bar properties evolve over 8 Gyr at 1 Gyr intervals.

2.2. Characterizing Bars and $f_{\rm opt}$ Out to $z \sim 1.0$

Table 1 illustrates the two methods that we use for assessing bar properties in two redshift slices at $0.25 < z \leq 0.70$ and $0.7 < z \leq 1.0$. The first method (referred to as Method I in Table 1) is to identify bars in the reddest filter (F850LP) at all z in order to minimize extinction and better trace old stars. However, with this method, the rest-frame bandpass shifts significantly, from I to B across the redshift range 0.2–1.0. The second complementary method is to trace bars in both F606W and F850LP images such that the rest-frame band remains relatively constant, between B and V, out to $z \sim 1.0$.

We identify bars and other galactic components in F606W and F850LP images via the widely used (e.g., Wozniak et al. 1995; Jogee et al. 1999, 2002; Knapen et al. 2000) procedure of fitting ellipses using the standard IRAF "ellipse" routine. We developed a wrapper that automatically runs "ellipse" for a range of different initial parameters, performing up to 200 fits per galaxy. We successfully fitted ellipses to 90% of the 1590 galaxies, while the 10% failure cases included mostly very disturbed systems where no centering could be performed and some extended low surface brightness systems. For all fitted galaxies, we inspected the image (Fig. 1a), the fitted ellipses overlaid on the images (Fig. 1b), and the radial profiles (Fig. 1c) of intensity, ellipticity (e), and position angle (P.A.) in order to confirm that the best fit is reliable. This inspection was aided by a visualization tool that we developed. We identify a bar as such if the fitted ellipses and radial profiles show the following characteristic bar signature (e.g, Wozniak et al. 1995) illustrated in Figure 1. (1) The ellipticity (e) must rise to a *global* maximum $e_{\rm max}$, which we require to be above 0.25, as well as above that of the outer disk, while the P.A. has a plateau (within $\pm 20°$) along the bar. (2) Beyond the bar end, as the bar-to-disk transition occurs, e must drop by ≥ 0.1, while the P.A. usually changes by $\geq 10°$. From the profiles, we identify e, P.A., and semimajor axes a of both the bar and the outer disk. We quantify the bar strength using $e_{\rm max}$, which correlates
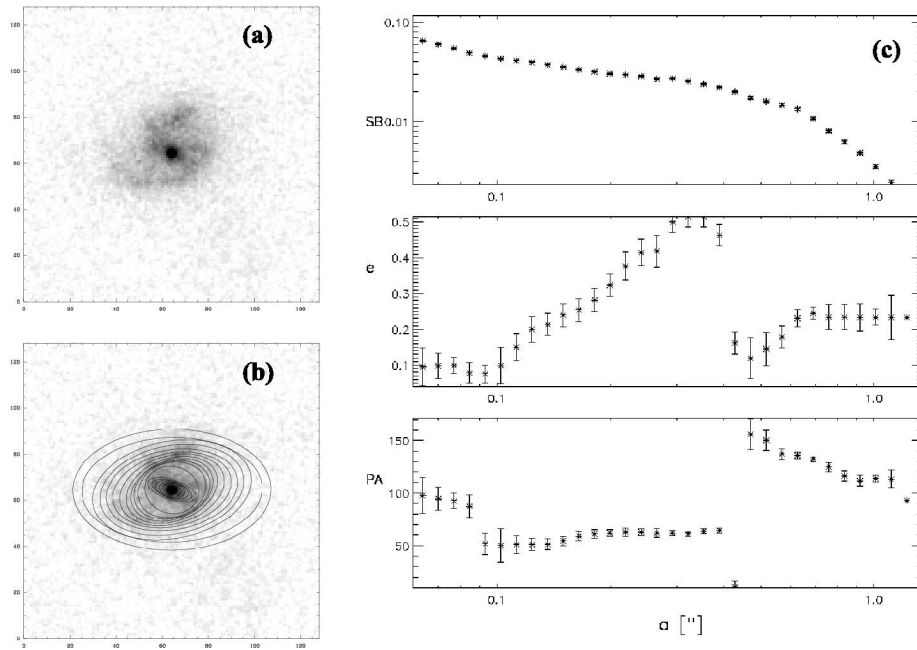
FIG. 1.—Characterization of bars out to $z \sim 1.0$: The GEMS image of a $z \sim 0.5$ galaxy with a bar, prominent spiral arms, and a disk is shown (*a*) without and (*b*) with an overlay of the fitted ellipses. (*c*) In the resulting radial plots of the surface brightness, ellipticity *e*, and P.A., the bar causes *e* to rise smoothly to a global maximum, while the P.A. has a plateau. Beyond the bar end ($a \sim 0\farcs36$), the spiral arms lead to a twist in P.A. and varying *e* before the the disk dominates.

locally with other measures of bar strength, such as the gravitational bar torque (Laurikainen et al. 2002).

The sample of 1430 galaxies with successful ellipse fits includes galaxies of different morphological types (disks and spheroids), inclinations, and absolute magnitudes. We apply two cuts at $M_V \leq -19.3$ and -20.6. The first cut gives us a sizeable sample of galaxies with a range of absolute magnitudes (-19.3 to -23.8) similar to that of the Ohio State University (OSU) survey, which is used to define the local bar fraction (ESO2). However, *K*-corrections based on local Scd templates (Coleman et al. 1980) suggest that we are only complete out to $z \sim 0.8$ for the first cut. The second more stringent cut at -20.6 ensures completeness out to $z \sim 1.0$, but it reduces the sample drastically (see Table 1). In addition, to ensure reliable bar detection, we use the disk inclination *i* from ellipse fits (§ 2.2) to exclude highly inclined ($i > 60°$) galaxies.

The optical bar fraction f_{opt} is defined as ($N_{bar}/N_{sp/disk}$), where $N_{sp/disk}$ is the number of spiral or disk galaxies and N_{bar} is the number of such systems hosting bars. We identify spiral/disk

galaxies using three independent techniques (Table 1). We first use the criterion $n < 2.5$, where *n* is the index of single-component Sersic models fitted to GEMS galaxies (B. Häussler et al. 2004, in preparation) with the GALFIT (Peng et al. 2002) package. Our choice of $n < 2.5$ is dictated by the fact that a study of GEMS galaxies at $z \sim 0.7$ (Bell et al. 2004), as well as tests in which we insert artificial galaxies in the GEMS fields, suggest that a Sersic cut of $n \leq 2.5$ picks up disk-dominated systems. The second technique uses a cut $C < 3.4$, where *C* is the CAS (Conselice et al. 2000) concentration index. Third, we use rest-frame $U - V$ color cuts in the range 0.8–1.2 to broadly separate spiral galaxies from red E/S0s, based on local SED templates and the observed red sequence at $z \sim 0.7$ (Bell et al. 2004).

3. RESULTS AND DISCUSSION

The bars that we identify primarily have ellipticities $e \geq 0.4$ and semimajor axes *a* in the range $0\farcs15$–$2\farcs2$ and 1.2–13 kpc (Fig. 2). Our experiment of artificially redshifting *B*-band images
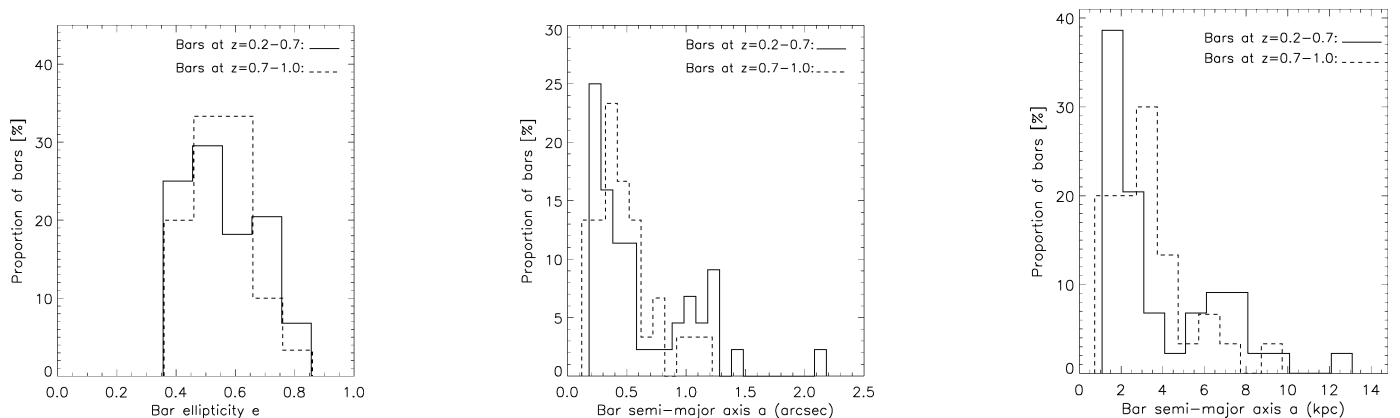

FIG. 2.—Comparison of bars out to look-back times of 8 Gyr. The bar ellipticity *e* (*left*) and semimajor axis *a* in arcseconds (*middle*) and kiloparsecs (*right*) are shown for bright ($M_V \leq -19.3$), moderately inclined ($i < 60°$) galaxies at $z \sim 0.2$–0.7 ($T_{back} \sim 2$–6 Gyr) and $z \sim 0.7$–1.0 ($T_{back} \sim 6$–8 Gyr). The bars identified are primarily strong, with $e \geq 0.4$. A large fraction have $a < 0\farcs5$, and their detection is aided by the narrow ACS PSF.

of a subset of OSU galaxies out to $z \sim 1$ shows that it is difficult to unambiguously identify weaker ($e \leq 0.3$) bars, and we limit the discussion in this Letter to strong ($e \geq 0.4$) bars. Table 1 shows the optical bar fraction f_{opt} of such bars in the two redshift slices ($0.25 < z \leq 0.70$ and $0.7 < z \leq 1.0$) derived in the reddest filter and in a relatively fixed rest-frame band (§ 2.2). Results for $M_V \leq -19.3$ are shown, based on 627 galaxies out of which we identify 258 moderately inclined ($i < 60°$) spirals that host ~80 bars. The consistency in the six entries attests to the robustness of the results and shows that the fraction of optically visible bars remains in the range 23%–36% or at ~30% ± 6% in both slices. Incompleteness effects (§ 2.2) do not bias the results since the cut at -20.6 gives similar bar fractions, shown in brackets (Table 1). The bar fraction is slightly higher in the rest-frame I band than B band, possibly indicative of dust and star formation masking bars at bluer wavelengths. Our findings of a fairly constant f_{opt} are consistent with E04 and do not show the dramatic decline in f_{opt} reported by A99.

More than 40% of the bars that we detect have semimajor axes $a < 0\farcs5$ (Fig. 2), and many of these smallest bars may have been missed in earlier WFPC2 (e.g., A99) and NICMOS studies that did not benefit from the small ($0\farcs05$) ACS pixels and the resulting narrow PSF. In addition to the wider WFPC2 PSF, cosmic variance, low number statistics, and methodology may have led to the lower f_{opt} reported by A99, but we cannot address this issue further here, as the coordinates of galaxies in that study have not been published.

How do our results compare to f_{opt} for correspondingly strong bars in the local universe? There are as yet no statistics published on $z \sim 0$ bars based on a large volume-limited sample such as the Sloan Digital Sky Survey. As the next best alternative, we turn to the OSU sample (E02). For $i < 60°$ spirals, we find $f_{opt} \sim 37\%$ for strong bars classified according to the visual RC3 "SB" bar class and $f_{opt} \sim 33\%$ for strong bars classified according to $e \geq 0.4$, where e is based on ellipse fits to OSU B-band images. Thus, it appears that the optical fraction of strong ($e \geq 0.4$) bars remains remarkably similar at ~30%–37% from the present day out to look-back times of 2–6 Gyr ($z \sim 0.2$–0.7) and 6–8 Gyr ($z \sim 0.7$–1.0).

Our findings have several implications for disk and bar evolution. (1) The abundance of strong bars at early times implies that dynamically cold disks that can form large-scale stellar bars are already in place by $z \sim 1$. They also suggest that highly triaxial, centrally concentrated DM halos, which tend to destabilize the bar (El-Zant & Shlosman 2002), may not be prevalent in galaxies at $z \sim 0$–1. (2) The remarkably similar fraction of strong bars at look-back times of 6–8 Gyr, 2–6 Gyr, and in the present day supports the view that large-scale stellar bars are long-lived (e.g., Athanassoula 2002; Shen & Sellwood 2004; Martinez-Valpuesta et al. 2004), with a lifetime well above 2 Gyr. The alternative option, statistically allowed by the data, is that the combined destruction and reformation timescale of bars is on average well below 2 Gyr. However, this is highly implausible because the destruction of a bar leaves behind a dynamically hot disk that cannot reform a bar unless it is substantially cooled via processes that take at least several Gyr, such as the accretion of large amounts of cold gas. (3) We note that a similar *fraction* of bars at different epochs does not exclude the possibility that the bar strength (ellipticity) and its size can evolve in time because of intrinsic factors and concurrent changes in the surrounding disk, bulge, and halo potentials (e.g., Athanassoula 2002; Martinez-Valpuesta & Shlosman 2004). Kolmogorov-Smirnov tests on the distributions of e and a for different magnitude cuts yield primarily P in the range 0.2–0.5, where P is the significance level for the null hypothesis that the two data sets are drawn from the same distribution. Such values of P hint at evolutionary effects, but a larger sample is needed to draw definite conclusions. While this Letter focuses on the optical bar *fraction*, in Paper II we will invoke the full GEMS sample of 8300 galaxies to compare bar and host galaxy properties (e.g., disk scale lengths, masses, and B/D ratios) over the last 8 Gyr at 1 Gyr intervals.

REFERENCES

Abraham, R. G., Merrifield, M. R., Ellis, R. S., Tanvir, N. R., & Brinchmann, J. 1999, MNRAS, 308, 569 (A99)
Athanassoula, E. 2002, ApJ, 569, L83
Bell, E. F., et al. 2004, ApJ, 600, L11
Benítez, N., et al. 2004, ApJS, 150, 1
Bournaud, F., & Combes, F. 2002, A&A, 392, 83
Coleman, G. D., Wu, C.-C., & Weedman, D. W. 1980, ApJS, 43, 393
Conselice, C. J., Bershady, M. A., & Jangren, A. 2000, ApJ, 529, 886
Elmegreen, B. G., Elmegreen, D. M., & Hirst, A. C. 2004, ApJ, 612, 191 (E04)
El-Zant, A., & Shlosman, I. 2002, ApJ, 577, 626
Eskridge, P. B., et al. 2002, ApJS, 143, 73 (E02)
Friedli, D., & Benz, W. 1993, A&A, 268, 65
Hunt, L. K., & Malkan, M. A. 1999, ApJ, 516, 660
Jogee, S., Kenney, J. D. P., & Smith, B. J. 1999, ApJ, 526, 665
Jogee, S., Scoville, N. Z., & Kenney, J. 2004a, ApJ, submitted (astro-ph/0402341)
Jogee, S., et al. 2002, ApJ, 570, L55
———. 2004b, in Penetrating Bars through Masks of Cosmic Dust, ed. D. Block, K. Freeman, R. Groess, I. Puerari, & E. K. Block (Dordrecht: Kluwer), in press (astro-ph/0408267)

Knapen, J. H., Shlosman, I., & Peletier, R. F. 2000, ApJ, 529, 93
Kormendy, J. 1982, in Morphology and Dynamics of Galaxies, ed. L. Martinet & M. Mayor (Sauverny: Obs. Geneve), 113
Kormendy, J., & Kennicutt, R. C., Jr. 2004, ARA&A, 42, 603
Laurikainen, E., Salo, H., & Rautiainen, P. 2002, MNRAS, 331, 880
Martinez-Valpuesta, I., & Shlosman, I. 2004, ApJ, 613, L29
Martinez-Valpuesta, I., Shlosman, I., & Heller, C. H. 2004, ApJ, submitted
Peng, C. Y., Ho, L. C., Impey, C. D., & Rix, H. 2002, AJ, 124, 266
Pfenniger, D., & Norman, C. 1990, ApJ, 363, 391
Regan, M. W., Vogel, S. N., & Teuben, P. J. 1997, ApJ, 482, L143
Rix, H., et al. 2004, ApJS, 152, 163
Sakamoto, K., et al. 1999, ApJ, 525, 691
Shen, J., & Sellwood, J. A. 2004, ApJ, 604, 614
Sheth, K., Regan, M. W., Scoville, N. Z., & Strubbe, L. E. 2003, ApJ, 592, L13 (S03)
Shlosman, I., Frank, J., & Begelman, M. C. 1989, Nature, 338, 45
Shlosman, I., & Noguchi, M. 1993, ApJ, 414, 474
Wolf, C., et al. 2004, A&A, 421, 913
Wozniak, H., et al. 1995, A&AS, 111, 115